Journal of New Technology and Materials
JNTM
Vol. 04, N°01 (2014)11-14

OEB Univ. Publish. Co.

Nanostructured metallic oxides coating

Mostefa Benhaliliba

Department of Material Technology, Physics Faculty, USTOMB University, BP1505 Oran, Algeria.

Received: 30 April 2014, accepted 26 May 2014

Abstract

This project has been focused on structural, morphological, optical and photoluminescence properties of pure ZnO thin film. Here, zinc oxide thin films are grown on glass via facile and low cost sol gel spin coating process @ fixed spinning speed of 1000 RPM. The X-ray patterns, the transmittance, the particle size by the atomic force microscope are investigated. The particle size is equal to 120 nm and the surface roughness is found to be 23.33 nm. The photoluminescence analysis reveals near band emission and strong visible emission 2.11 and 2.80 eV.

Keywords: Spin coated ZnO films; X-rays pattern; transmittance; photoluminescence; SEM; TEM; Electron diffraction; AFM.

1. Introduction

Nowadays, zinc oxide (ZnO) film is the most studied material due to its various properties such as high transmittance in visible range, direct band gap around 3.3 eV, high exciton binding energy of 60 meV [1]. Zinc oxide was prepared by many techniques such as sol gel spin coating [2], spray pyrolysis deposition (SPD) [3-4], sputtering [5] and chemical vapor deposition CVD [6]. We use the sol gel spin coating as film deposition technique because it is low cost, facile, rapid, unobtrusive and environmental process. All these prompted features of this multifunctional material, attract many researchers to use it in many applications like sensors, light emitting diodes, piezoelectric and catalytic devices. Here, ZnO nanostructures are achieved by facile sol gel route. ZnO nanostructures have been successfully prepared in several morphologies like nanorods and nanowires [7-8]. This paper consists on detailed study of the structural, surface morphology, optical, photoluminescence properties of zinc oxide grown onto glass by a facile spin coating route. Furthermore ZnO nanorods were successfully synthesized and investigated by high resolution field emission transmission electron microscope (FE-TEM), electron diffraction, field emission scanning electron microscope (FE-SEM) and electron dispersive X-rays analysis (EDX) and atomic force microscope (AFM) analysis.

2. Experimental details

The ZnO films are produced by sol gel spin coating route. The substrate used is a microscope glass slides 76 x 26 mm supplied by object trager Isolab. 0.5 Molar of dehydrated zinc acetate ($Zn(CH_3COO)_2.2(H_2O)$), (99.5 %) supplied by Carlo Erba reagents, is dissolved in 10 ml of 2-Methoxyethanol stirred at 60°C for 10 mn and then 0.3 ml of the mono-ethanolamine (MEA) as stabilizer is added drop by drop, the clear solution is then obtained, the stirring continued for 1 hour. Consequently, the solution followed an ageing process for one day. Initially, the glass substrates were cleaned by a soft soap solution, washed systematically with the distilled water, then with ethanol in ultrasonic cleaner and finally were dried with argon. Using a micropipette the obtained gel was homogenously poured, on the substrate deposited on plates of spin coater (MTI, EQ-TC-100 desk-top type). The sample spins for one minute at 1000 RPM (rotate per minute); the sample is instantly heated at 150 °C for 10 mn. The process is repeated 5 times; finally the film is annealed at 400 °C for 1hour under air in furnace. In that way, the coated films are investigated by Shimadzu 3600 PC double beam UV-VIS-NIR spectrometer, the surface morphology is analyzed by the mean

of field emission scanning electron microscope JEOL JSM 7001F FE-SEM, the films are also examined by transmission electron microscope JEOL JEM 2100F FE-TEM and the chemical analysis of films is given by electron energy dispersive X-ray (EDX) spectrometers. Furthermore, morphology is explored by atomic force microscope Park system XE-100E Non contact cantilever Si used 256x256 pixels. Room temperature photoluminescence characterization is carried out using an experimental setup consisting of: a 325 nm 15 mW He-Cd laser (Kimmon), a 0.85 m double monochromator (SPEX, model 1404), and a GaAs photon counting photomultiplier (Hamamatsu). The range explored is from 350 to 600 nm, in 0.5 steps and a speed of 0.2 seconds/measured point.

3. Results and discussion

3.1. Structural properties investigation

The X-ray diffraction pattern for zinc oxide film recorded at room temperature is shown in Fig.1. The strong peak, well known (002) located at 2θ=34.42°, given by JCPDS card N° 36-1451 is displayed by a red dash line as depicted in figure 1. The as-grown films were identified as polycrystalline ZnO with a wurtzite crystal structure and preferred orientation along the (002) plane. As can be seen in X-rays spectra, film exhibits a polycrystalline structure and most of peaks are broadened. Since base of peaks are enlarged, the full width at medium height (FWMH) increases and grain size G, expressed as follows, is reduced [4];

$$G = \frac{K\lambda}{\beta \cos\theta} \qquad (1)$$

Where K is constant estimated at 0.94, λ is the wavelength of the X-ray used 1.54 Å, β is the full width at half maximum (FWHM) which has maximum intensity and 2θ is the Bragg angle.

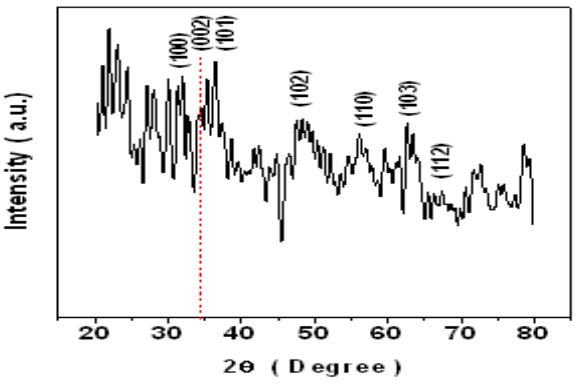

Figure 1: X-rays pattern of zinc oxide at room temperature; two-theta range is 20°-80°. Red dash line locates the peak (002) at 34.42 °.

According the (002) orientation, the grain size G is about 120 nm, the reticular distance d is of 0.26 nm and the textural coefficient is 1.1.

3.2. Microscopy observation

The AFM micrographs reveal that zinc oxide exhibit the nanorods which have grown according to z-axis direction as shown in figure 2. This result is confirmed by SEM observation (see figures 2 and 3). All elements analyzed are normalized as described in EDX as listed in table 1, Zn occurrence is obviously indicated, silicon may come from substrate glass, insignificant amounts of calcium (Wollastonite, $CaSiO_3$) and magnesium (MgO) are present respectively as impurities in starting precursor. The Honeycomb architectures are apparent in picture having diameter found to be 10 nm (as indicated by red arrow). It is confirmed that FE-TEM picture exhibits regular inner of sample and very slight pores density. Electron diffraction pattern show spots which located according to X axis and Y axis , the scale is 50 nm (see the fig 3 top). The Honeycomb architecture is visible at the higher magnification image shown in figure 3 (bottom). 3D-AFM picture shows evidently nanorods which grown one beside each other perpendicular to substrate surface as depicted in figure 4.

3.3. Optical Characterization

Figure 5 shows the dependence of transmittance T (%) and reflectance R (%) on incident photon wavelength which ranges within 200-2500 nm. T increases rapidly in UV spectrum, and reaches up to 86 % in visible range, as depicted inset of figure 5, and then varies slightly between 82 and 93% both in VIS and IR spectra. Reflectance attains 9.5 % at 384 nm, but it still minor in the whole photon wavelength range. The band gap energy of the ZnO films can be determined by the following relation,

$$(\alpha h\nu)^2 = h\nu - E_g \qquad (2)$$

Where E_g (eV) is the optical band gap, α (m^{-1}) is the absorption coefficient and ν (Hz) is the photon frequency. Figure 6 depicts how the direct energy gap of the coated film has been estimated by extrapolating the linear part of $(\alpha h\nu)^2$ plot versus photon energy to the wavelength axis. It found to be 3.26 eV, which agrees well with our previous result [1-4].

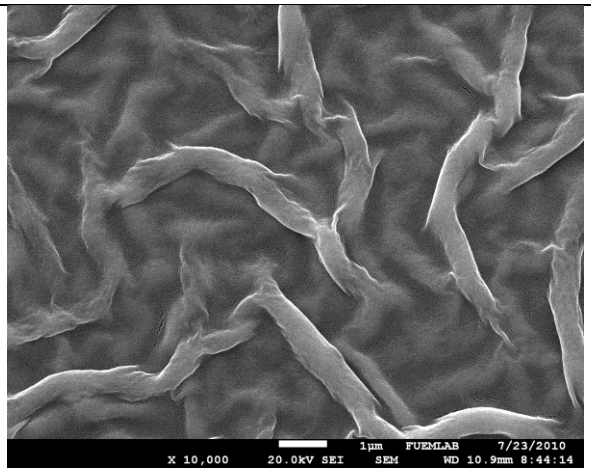

Figure 2: Field effect scanning electron microscope (FE-SEM) picture at low magnification (x10 000, 20KV) (top), EDX spectrum is displayed (bottom).

Element	App Conc.	Intensity Corrn.	Weight%	Weight% Sigma	Atomic%
C K	1.15	0.2796	2.89	0.34	5.64
O K	53.67	0.9078	41.55	0.33	60.92
Mg K	1.06	0.5516	1.35	0.07	1.30
Si K	27.00	0.7730	24.54	0.20	20.50
Ca K	6.21	0.9854	4.43	0.08	2.59
Zn K	29.80	0.8297	25.24	0.30	9.06
Totals			100.00		

Table 1. EDX analysis results of ZnO film produced @ 1000 RPM.

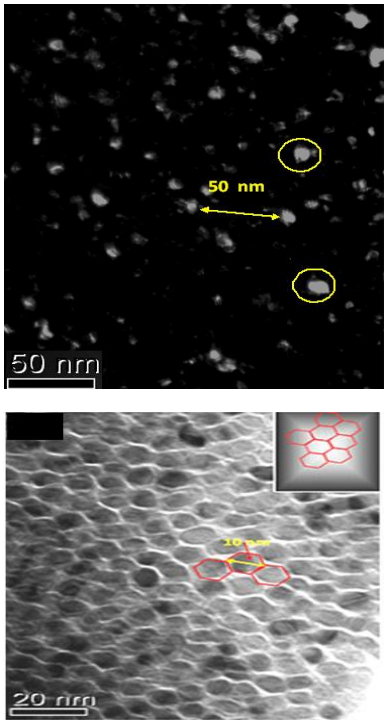

Figure 3. A high-resolution TEM image and an electron diffraction pattern obtained for coated sample ZnO produced at 1000 RPM (top), bright field TEM image (bottom).

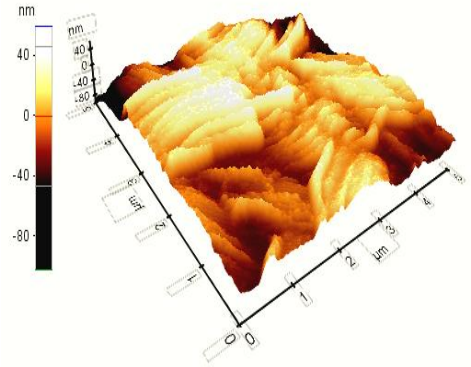

Figure 4. 3D-AFM view of spin coated ZnO film.

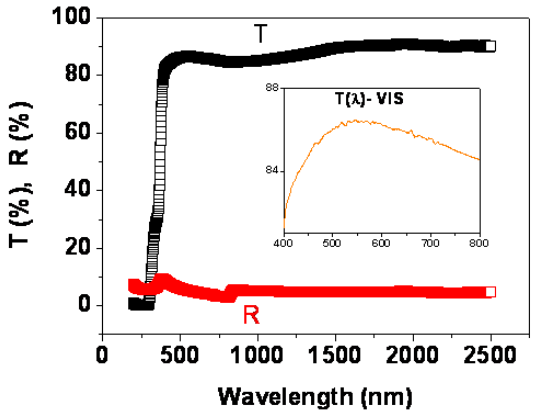

Figure 5. Transmittance (balck curve) and Reflectance (red curve) plots against photon wavelength of spin coated ZnO film, inset shows the transmittance in visible range.

3.4. Photoluminescence analysis

The optical properties of the coated zinc oxide films nanorods are examined using photoluminescence at room temperature as shown in figure 7. PL spectrum exhibits various emission bands, including strong near band edge emission peak located respectively at 442 nm (2.80eV) which corresponds to blue emission. This emission peak may prove that ZnO nanorods have high cristallinity. Others peaks of low intensity located at 447nm -538nm (2.77eV-2.30eV), which correspond respectively to green band emission. These bands might due to defects occurrence such as oxygen traps.

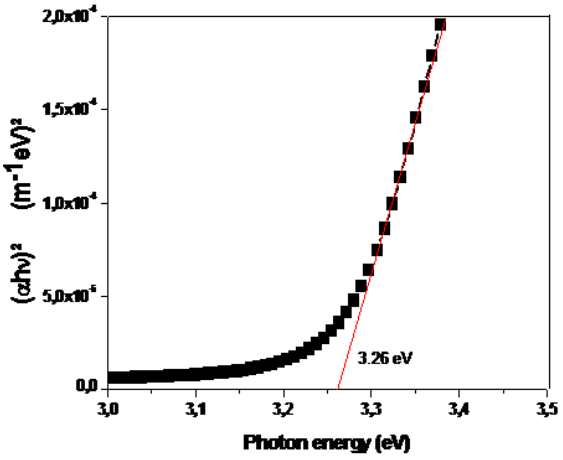

Figure 6. Absorbance variation versus photon wavelength of spin coated ZnO film, optical band gap, Eg= 3.26 eV, is deduced.

ZnO exhibits the emission peaks with differents energies 2.11-2.82 eV as listed in table. The strong emission is apparent in visible spectrum. Photoluminescence spectrum shows near band edge NBE and defects emissions. The Gaussian deconvolution ascribed the strong PL peaks to the following positions: 587.73±0.02 nm (2.11 eV), 534.38±0.59 nm (2.32 eV), 545.88±1.27 nm (2.27 eV) and 433.46±2.57 nm (2.86 eV).

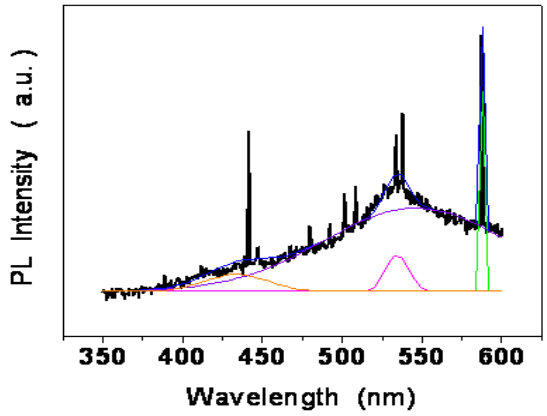

Figure 7: Room temperature photoluminescence spectra of undoped ZnO against wavelength (300-600 nm), curves of deconvolution fitting are displayed.

4. Conclusion

Zinc oxide nanorods were successfully synthesized by facile sol gel spin coating route. It reveals that zinc oxide was present in high amount in coated film by XRD pattern and EDX analysis. These ZnO nanorods were high transparent in VIS and IR ranges. SEM and TEM images reveal clusters presence at nanoscale, and the Honeycomb architecture is observed at high magnification. Stron visible emissions are detected by PL investigation.

Acknowledgements

The work, under contract number **D01920120039**, is included in project CNEPRU supported by the Algerian High Level Teaching and Scientific Research Ministry MESRS and Oran Sciences and Technology University USTOMB. The author would like to acknowledge the generous assistance of Mr. U. Akgül, FUMELAB laboratory, Firat University Turkey, for their fruitful help in performing SEM observations.

References

[1] C. Aydın & M. Benhaliliba & Ahmed A. Al-Ghamdi & Zarah H. Gafer & Farid El-Tantawy & F. Yakuphanoglu, J Electroceram. **DOI 10.1007/s10832-013-9829-5, (2013)**

[2] M. Benhaliliba, C.E. Benouis, A. Tiburcio-Silver, Y.S. Ocak, EPJ Web of Conferences, DOI: 10.1051/Owned by the authors, published by EDP Sciences, 2013,epjconf/201 **44** 03003 (2013) 34403003.

[3] M. Benhaliliba, C.E. Benouis, Z. Mouffak, Y.S. Ocak, A. Tiburcio-Silver, M.S. Aida, A.A. Garcia, A. Tavira, A. Sanchez Juarez, Superlattices and Microstructures 63 (2013) 228–239.

[4] M. Benhaliliba, C. E. Benouis, M. S. Aida , F. Yakuphanoglu, A. Sanchez Juarez, J Sol-Gel Sci Technol (2010) 55:335–342 DOI 10.1007/s10971-010-2258-x

[5] Y.S. Ocak, J. Alloys Compd., 513 (2012) 130-134.

[6] X. Li, Y. Yan, T.A. Gessert, C.L. Perkins, D. Young, C. DeHart, M. Young, T.J. Coutts, J. Vac. Sci. Technol. A 21 (3)
(2003) 1342–1346.

[7] Hoang-Si Honga, Gwiy-Sang Chung, Sensors and Actuators B195 (2014) 446–451.

[8]Y. Abdi, S.M. Jebreiil Khadem, P. Afzali, Current Applied Physics 14 (2014) 227-231.